C. R. Mecanique 340 (2012) 349–358

Contents lists available at SciVerse ScienceDirect

Comptes Rendus Mecanique

www.sciencedirect.com

Recent Advances in Micromechanics of Materials

Recent advances in spatiotemporal evolution of thermomechanical fields during the solid–solid phase transition

Q.P. Sun [a,*], H. Zhao [b], R. Zhou [a], D. Saletti [b], H. Yin [a]

[a] Department of Mechanical Engineering, The Hong Kong University of Science & Technology, Hong Kong, China
[b] Laboratoire de mécanique et technologies (LMT-Cachan), ENS-Cachan/CNRS-UMR 8535/Université Paris 6, 94235 Cachan cedex, France

ARTICLE INFO

Article history:
Available online 4 April 2012

Dedicated to Prof. André Zaoui on the occasion of his 70th birthday

Keywords:
Phase transition
NiTi shape memory alloy
Self-organization and collective behavior
Domain patterns and domain spacing
Strain rate
Temperature and stress oscillations
Cyclic deformation
Effect of time scales

ABSTRACT

This article reports recent advances in the micromechanics experimental research of the solid–solid phase transition in NiTi shape memory alloys. In the first part, we show how an initially macroscopic homogeneous material state becomes unstable and transforms into a new phase under external driving, leading to the emergence of macroscopic spatial periodic self-organized domain patterns and their loading rate dependence. In the second part, we report the phenomenon of temperature and stress oscillations under cyclic phase transition. We elucidate the multi-physical and multi-scaled nature of the spatiotemporal evolution of thermomechanical fields and emphasize and examine the important role of time scales and thermomechanical coupling in the response of the material.

1. Introduction

Phase transition phenomena in solids are of vital interest in research of solid mechanics, physics, materials sciences and engineering because materials with solid–solid phase transitions have important applications in many technical fields, especially with the fast development of nano-structured biomaterials and nano-technology. Nonlinearity, non-equilibrium and multi-field coupling are inherent in the solid–solid phase transition process and play a central role in properties and behaviors observed in many material systems [1–10]. This is because many processes in the fabrication and service of materials (e.g., solidification in casting of alloys, diffusion and displacive phase transitions, high speed metal forming and cutting, field-induced cyclic phase transition and vibration of structural components) are intrinsically thermodynamic non-equilibrium. They involve, at one stage or another, different versions of material nonlinearity, instability and multi-field coupling at different length and time scales and constitute the main physical origins of material heterogeneity and deformation patterns under non-equilibrium conditions.

Superelastic NiTi shape memory alloys (SMAs) are increasingly used in many fields, from biomedical human artificial joints to small-scale sensors and actuators in micro-electro-mechanical-systems (MEMS), and to the vibration and damping control devices in small and large scale engineering structures. These applications utilize the material's large reversible deformation and damping capacity due to reversible transformation between austenite and martensite phases. The response of the material in both monotonic and cyclic transformations under different frequency and amplitudes of tensile loading is closely related to the fatigue and degradation of the devices and therefore is always a key concern in the application. One of the unique aspects in the phase transition behavior of the NiTi under tension is the self-organized formation of the

* Corresponding author.
E-mail address: meqpsun@ust.hk (Q.P. Sun).

1631-0721/$ – see front matter
doi:10.1016/j.crme.2012.02.017

macroscopic localized transformation domain (band) and its subsequent evolution. When stretched under uniaxial tension, the material transforms collectively by formation and growth of macroscopic domains and the domain patterns exhibited strong loading rate dependence [4–8,11–25]. This is because the domain evolution in the phase transition of the material is an intrinsically thermomechanical coupled process. On the one hand, the domain front propagation is accompanied by heat release and heat transfer which makes the process deviate from isothermal condition. On the other hand, the stress–strain response in phase transition and the created thermal field are coupled, since according to the Clausius–Clapeyron relation, the transformation stress is temperature-dependent [26]. Another important aspect of the material is that, when subjected to cyclic deformation, the heat generation and exchange between the specimen and the environment strongly depend on the deformation frequency. Preliminary investigations showed that the thermomechanical responses of the material exhibit distinctive temperature and stress oscillations. The amplitudes of the oscillations vary significantly with the deformation frequency and can even damage the material before the oscillations reach steady state. From both academic and practical points of view, a comprehensive understanding of the coupling effect and roles of time scales in the response of NiTi over wide range of loading frequencies (strain rates) is required. Unfortunately, these important aspects remain much less explored and understood experimentally. Systematic, well controlled and instrumented experiments play a critical role in comprehending and quantitative modeling such multi-scaled phenomena.

From theoretical point of view, phase transitions in NiTi polycrystals are first order transformation events with nucleation and growth of microscopic domains at grain size level. Furthermore, for fine-grained polycrystalline NiTi SMAs, the phase transitions at microscopic level can take place collectively, leading to the meso- or macroscopic level formation and growth of localized transformation domains. The generation and transfer of hysteresis dissipative heat and latent heat can lead to swift temperature variations of the specimen, heat conduction within the material and heat convection with the ambient environment. However, quantifying the thermomechanical responses and identifying the roles of external and internal governing parameters in the rate-dependent response is more challenging experimentally than measuring conventional quasi-static isothermal mechanical properties. First, the domain morphology under high-strain rate loading must be captured by a high speed camera with sufficient spatial resolution. Second, the transient temperature variations of the specimen in cyclic phase transitions must be measured with sufficient time resolution. Third, temperature variations and the stress–strain responses of the material depend strongly on the test conditions (such as particular specimen geometry and the ambient conditions) which must be well controlled. Different specimen size and the surrounding ambient environment can lead to different test results. Finally, to have a clear picture of the physical process, the measurements of mechanical and thermal quantities need to be synchronized. Special loading and measurement facilities need to be developed to meet these challenges.

This article reports recent experimental work by the authors on the spatiotemporal evolution of thermomechanical fields during the solid–solid phase transition of NiTi shape memory alloys under both monotonic and cyclic tensile loading of different rates in stagnant air. In Section 2, we report the rate-dependent domain patterns in strip specimen and show how an initially macroscopic homogeneous deformation state of austenite phase becomes unstable and transforms to martensite under external stress, leading to the emergence of meso-scale and near spatially periodic self-organized domain patterns. The roles of the phase transition time and the heat transfer time scales in the material's behavior under a wide range of loading rates are examined. In Section 3, we report the phenomenon of temperature and stress oscillations under cyclic phase transition by the synchronized measurement of the temperature and stress–strain histories of the specimen. We discuss the physical origin of the phenomena and examine the important role of time scales and thermomechanical coupling in the material behavior. Results of theoretical analysis will be briefly reported in parallel to help understand the phenomena. We give conclusions in Section 4.

2. Rate-dependent deformation patterns of a superelastic NiTi SMA strip

In this section, we report the experimental results of the stretching rate effect (nominal strain rate) on the domain patterns in a nano-structured polycrystalline NiTi SMA strip in room-temperature still air. The geometry of the superelastic NiTi strip is shown in Fig. 1(a). The alloy composition, grain size, transformation temperature, latent heat and the specimen preparation are given in Refs. [17,18,21–23]. The characterization of the isothermal tensile stress–strain curves of the material at different constant temperatures and the temperature dependence of both nucleation stress of the meso-domain (see the peak stress in Fig. 1(b)) and propagation stress of the meso-domain (see the flat plateau stress in Fig. 1(b)) are shown in Figs. 1(b) and (c). A standard MTS hydraulic test machine (for the stretching rate of 10^{-4}/s–10/s) and custom-modified Split Hopkinson Tension Bar (for the stretching rate of 23/s–180/s) were used to transform the material over the stretching rate range of 10^{-4}/s–10^{2}/s in room-temperature (25 °C) air. The measurements of the nominal stress–strain curves and the macroscopic domain patterns at different strain rates were synchronized. Figs. 2(a) and (b) are the measured nominal stress–strain curves at different strain rates and the corresponding magnified domain patterns at the surface of the strip are shown in Fig. 2(c). The domain number density and the domain spacing over the gauge length are obtained from the recorded images and are summarized in Fig. 3. It was found that both the stress–strain response and the mode of deformation changed significantly with the loading rate. The nominal stress–strain curve changed from the near-isothermal plateau type with distinct stress drops at the very low stretching rate (10^{-4}/s) to the hardening type (3.2×10^{-4}/s–10/s, and 23/s–180/s). The domain number (spacing) increased (decreased) monotonically with the stretching rate (see Figs. 2(c) and 3), from a single macroscopic domain under very slow near-isothermal stretching at 10^{-4}/s, to many parallelepiped martensite

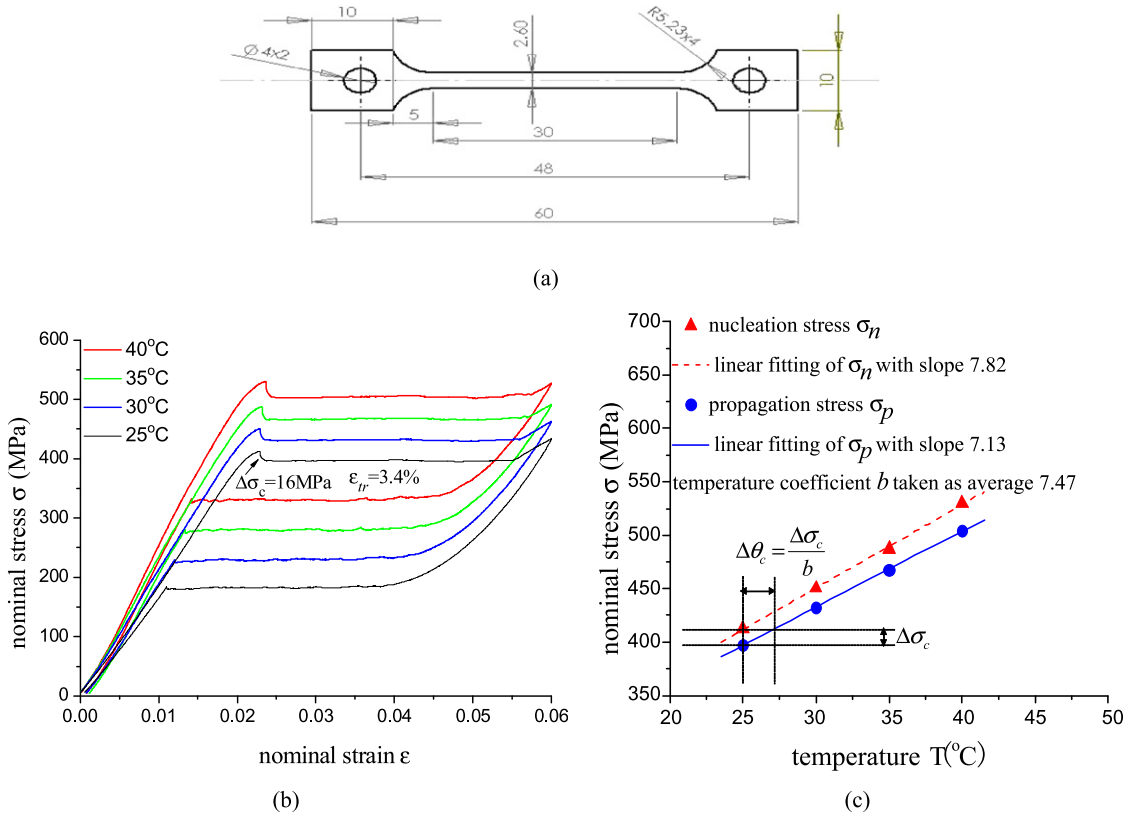

Fig. 1. (a) The geometry of the NiTi strip with thickness of 0.5 mm, (b) isothermal nominal stress–strain curves (at nominal strain rate of 10^{-5}/s) of the material in different constant temperatures, and (c) temperature dependence of both nucleation and propagation stresses obtained from (b).

domains (3.2×10^{-2}/s–10/s, see Fig. 2(c)), and eventually to the mode of multiple-nucleation of very fine martensite micro-bands (see the fine stripes in Fig. 2(c)) (at strain rates of 44/s–180/s). The domain spacing, as a measure of the deformation heterogeneity of the material during transformation, follows a power-law scaling with the applied stretching rate (see Fig. 3). Experimental videos on the morphology and temperature evolution of a NiTi strip by Q.P. Sun's group can be found at the website: http://www.me.ust.hk/~meqpsun/experimentvideos/.

The phenomena of the multiple domain formation in non-isothermal stretching of a superelastic polycrystalline NiTi strip can be traced back to the early work in 1990s [4–6,15]. The thermal effect and the thermomechanical coupling (a kind of feedback mechanism) on the stress–strain and domain patterns can be examined clearly [21] under nominal tensile strain rate $\dot{\varepsilon} = 3.3 \times 10^{-3}$/s as shown in Fig. 4 with the help of the property shown in Fig. 1(c). After an initial macroscopic homogeneous deformation (notice that at the end of the homogeneous deformation with nonlinearity in the stress–strain curve, a certain small amount of phase transition already took place at the microscopic level [5, 27]), two high-strain domains (one near the top and the other near the bottom tapered end) nucleated simultaneously with a stress drop (see patterns *a* and *b* in Figs. 4(a) and (b)). An instantaneous local heating of the domains due to the released latent heat can be detected by a thermal camera. In the subsequent growth of the two domains under continued stretching, the two fronts near the strip's tapered ends were soon arrested, which led to the speeding up of the other two fronts and a further temperature rise there. The increase in the front temperature in turn caused an increase in the applied stress to drive the fronts (*b*–*c* in Fig. 4(a)). When the applied stress reached the nucleation stress for the middle cooler untransformed region of the specimen, two new domains nucleated sequentially with stress drops (see *c*–*d* and *e*–*f* in Fig. 4). The subsequent propagation of the six fronts (*f*–*g* in Figs. 4(a) and (b)) was still accompanied by an increase in the front temperature and therefore the increase in the applied stress up to 413 MPa where the fifth domain nucleated (see *g*–*h* in Fig. 4). Because of the domain growth and heat conduction, the temperature of the specimen tended to become uniform and was higher than the initial temperature. The propagation stress for the fronts kept increasing with loading but was no longer higher than the nucleation stress of the warmed austenite, so there was no further domain nucleation in the continued stretching. Thus, the maximum number of martensite domains in this loading process under the strain rate 3.3×10^{-3}/s was five. With further loading the domains started to merge sequentially (see *j*–*m* in Fig. 4). Each merging was accompanied by a small stress drop and a reduction in domain number.

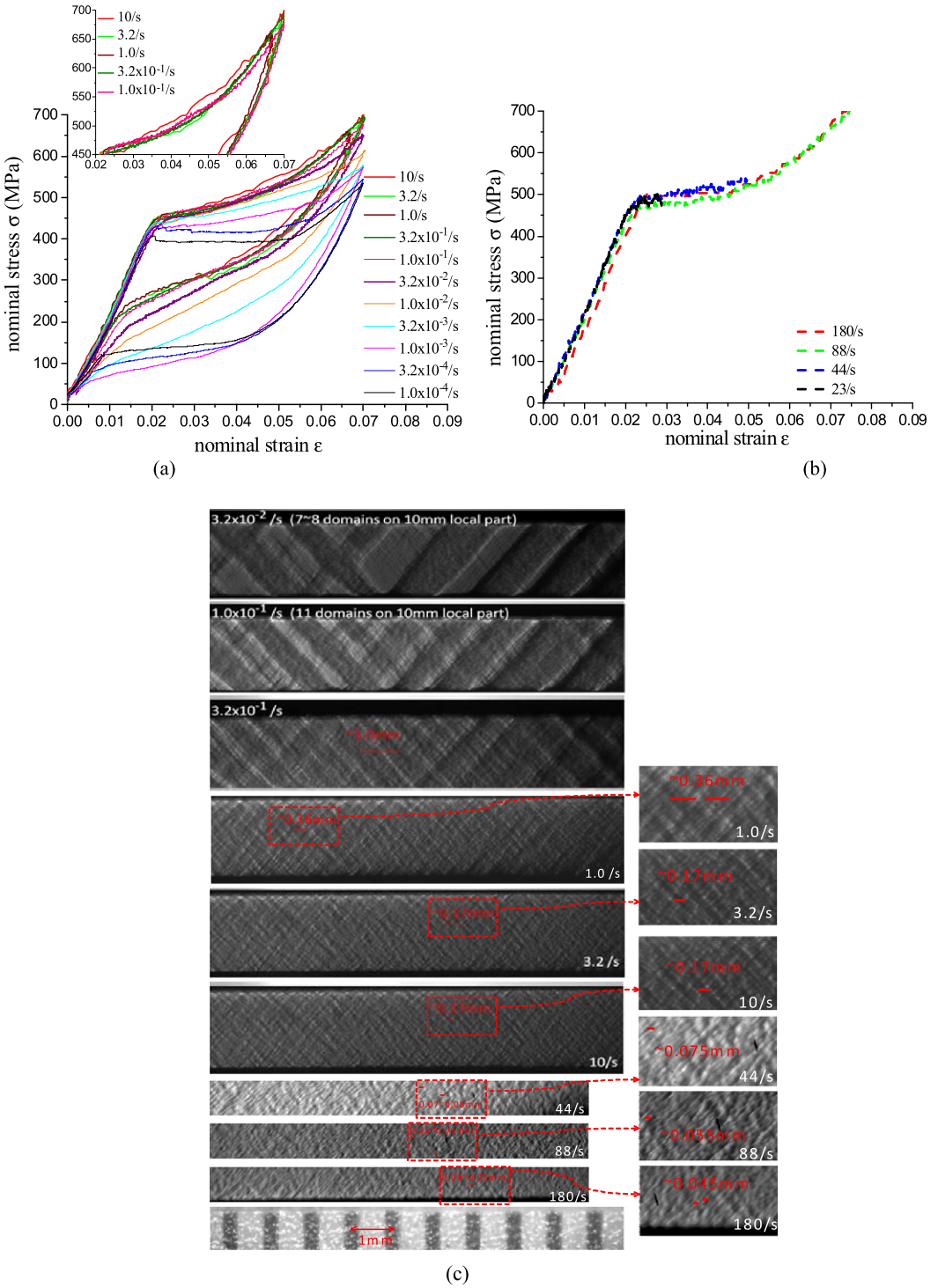

Fig. 2. (a) Stress–strain curves of the specimen in Fig. 1(a) under strain rates 10^{-4}/s–10/s and (b) 23/s–180/s, (c) the magnified domain patterns in the strip specimens under stretching rates from 3.2×10^{-2}/s to 180/s (at the same applied transformation strain of 2%, the left bottom photo in (c) is the photo of a plastic ruler as a scale bar for comparison).

From the above description, we can see that the created thermal and mechanical fields by the first order phase transformation in SMAs are intrinsically coupled in the sense that phase transition creates heat which in turn influence the stress since the stress required to transform the material is temperature-dependent (the Clausius–Clapeyron relation). It is this coupling that makes the stress–strain response and deformation pattern rate-dependent. The observed phenomenon

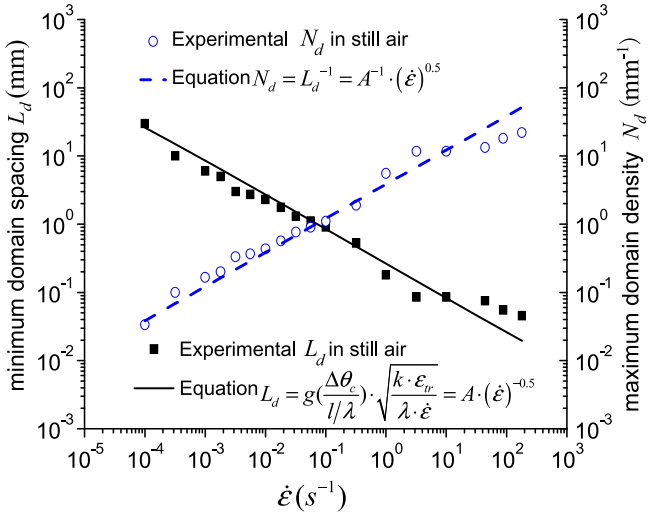

Fig. 3. The experimental data of the domain number density (domain spacing) and the comparison with the model predictions (Eqs. (1) and (2)).

involves, among other factors, the competition of loading time (or phase transition time or heat release time) and heat transfer time. We can roughly say that the observed "rate effect" is in fact a temperature or heat flow effect due to the deviation from the ideal isothermal condition. The rate effect would disappear as far as the testing can be controlled as isothermal [13,23].

The above physics underlying the rate dependence of the behavior [4–8,11–19] leads to the following important criterion of domain formation: as long as the applied stress (it is also the front propagation stress for the existing domains) is higher than the domain-nucleation stress at the coolest point of the untransformed region, new domains will nucleate. Such nucleation will repeatedly take place until there are sufficient domains in the specimen so that the above nucleation criterion is violated. As a result, each stretching rate corresponds to a maximum domain number (or minimum domain spacing). In principle, the higher the stretching rate, the less time to transfer the latent heat and therefore the more domains we observe. Based on this physical insight into the multiple-domain formation and thermomechanical coupling (feedback), modeling and analysis have been conducted recently [17,23]. It is revealed that the competition among the different time scales of loading (strain rate $\dot{\varepsilon}$, i.e., the rate of heat release), heat conduction (conductivity k) and convection (convective coefficient h) plays an important role in the above rate dependence of domain patterns. Using a simplified one-dimensional model, the effects of $\dot{\varepsilon}$, k and h on the domain number and spacing were identified. It is shown that for most real material properties of SMA and heat transfer boundary conditions, the domain number (domain spacing) increases (decreases) with increasing applied nominal strain rate $\dot{\varepsilon}$ and decreases (increases) with increasing heat convection (h) and conductivity (k). In addition to the above general trends, simple explicit power-law scaling relationship (with exponent -0.5) between the domain number density N_d (domain spacing L_d) and the strain rate is derived for the case of tensile test in static air [17,23] where the effect of convection is ignorable as compared with the effect of internal conduction (i.e., conduction dominated with $h = 0$, and the readers are referred to [23] for more general cases involving both convection and conduction):

$$N_d = \frac{N}{L} = \frac{1}{A} \cdot (\dot{\varepsilon})^{\frac{1}{2}} \quad \text{where } \frac{1}{A} = \sqrt{\frac{\lambda}{-4k \cdot \varepsilon_T \cdot \ln(1 - \frac{\Delta\theta_{critical} \cdot \lambda}{l})}} \tag{1}$$

$$L_d = \frac{L}{N} = A \cdot (\dot{\varepsilon})^{-\frac{1}{2}} \tag{2}$$

Both Eqs. (1) and (2) agree quantitatively well with the experimental data in stagnant air without any fitting parameters (see Fig. 3).

3. Thermomechanical responses of a superelastic NiTi wire under cyclic phase transition

The cyclic behavior of a superelastic NiTi SMA often shows a stabilized hysteretic response before significant damage and final failure occur [22,25,31,32]. Although our knowledge of the cyclic behavior of traditional materials has increased rapidly over the past decades, the behavior of NiTi under a cyclic phase transition is still much less explored and understood so far. Recent experiments by the authors [22] revealed that two mechanisms of different physical origin coexist and interact in reaching the stabilization.

The first mechanism is the isothermal or near-isothermal transformation-induced formation and saturation of complex dislocation structures and residual martensite in the grains of NiTi polycrystals during the cyclic trainings under tension as shown in Fig. 5 for a superelastic wire of 40 mm gauge length and 3.5 mm diameter in room-temperature (25 °C) air.

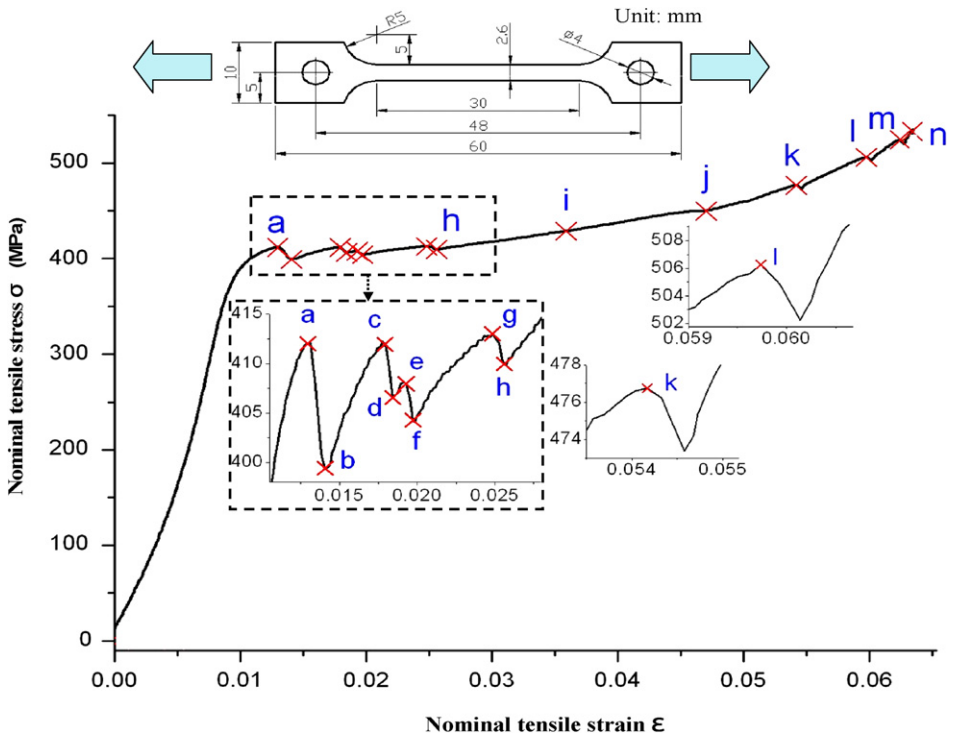

(a)

a b c d e f g h i j k l m n

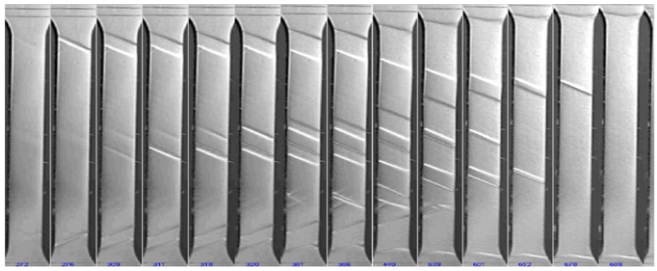

(b)

Fig. 4. Multiple-domain nucleation and growth in a NiTi strip under nominal strain rate of 3.3×10^{-3}/s: (a) the nominal stress–strain response; (b) the corresponding surface morphology.

Such plastic strain accumulation and saturation in isothermal phase transitions can lead to the mechanical saturation (or shake down) of stress–strain response with repeating hysteresis loops. In displacement-controlled cyclic phase transition of Fig. 5, such "shake down" is evidenced by a gradual decrease (∼100 MPa) and saturation in the applied stress and a gradual increase (∼1%) and saturation in the residual strain.

The second mechanism, being of thermal nature, is the release/absorption of transformation heat (the latent heat and the hysteresis heat) and heat transfer with the ambient. For a fresh specimen, this mechanism works interactively with the first mechanism in reaching the stabilized cyclic response of the material. In order to reveal the pure thermal effect, cyclic tests on the trained wire specimen of Fig. 5 were performed under cyclic deformation (6% of strain amplitude) of frequency 0.004, 0.04 and 1 Hz respectively (see Figs. 6 and 7) [22]. We show that this mechanism, even when working alone, can produce a distinctive frequency-dependent temperature shift and oscillation which in turn brings stress shift and oscillation since the phase transition stress is inherently temperature-dependent. It should be noted that, in the spirit of the lumped analysis method [24], here we have ignored the spatial heterogeneity of the temperature and what we measured is actually the average temperature over the gauge length and we will use it as the specimen's temperature.

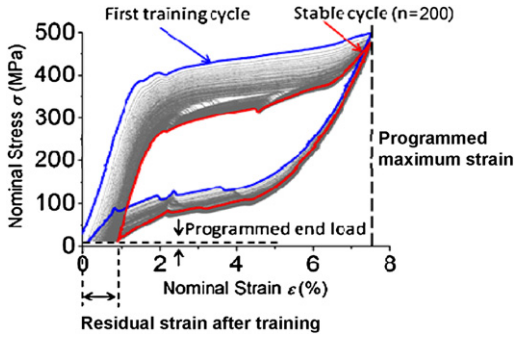

Fig. 5. The effect of the first mechanism on the stress–strain curves under cyclic phase transition.

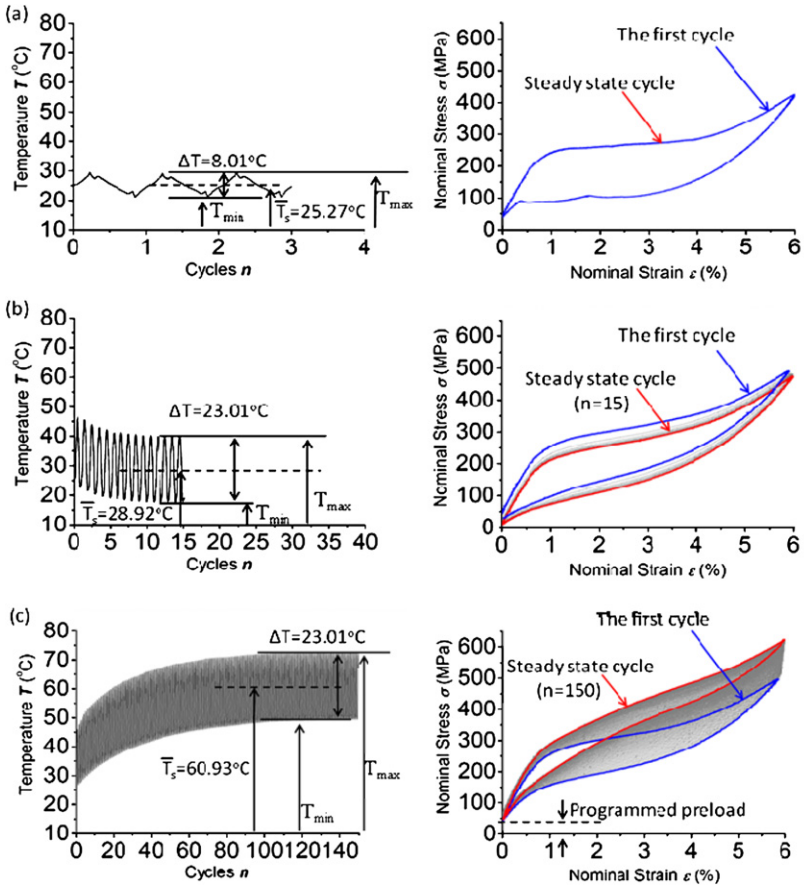

Fig. 6. Temperature and stress–strain evolutions under cyclic deformation frequency of: (a) 0.0007 Hz, (b) 0.04 Hz and (c) 1 Hz.

As shown in Fig. 6(a), for the cyclic loading frequency of 0.0007 Hz, the heat transfer via convection and conduction is much faster than the heat generation rate, so the thermal effect on the cyclic response is quite weak. The stress–strain curve is very close to that of the isothermal plateau type and the hysteresis loop area is mainly caused by the microscopic mechanical dissipative events [28] and represents a characteristic property of the polycrystalline material (see Fig. 6(a)).

At the intermediate cyclic loading frequency of 0.04 Hz, the combined effect of heat release and heat transfer becomes significant. Such thermal effect brings a strong non-isothermal and oscillating features to the cyclic behavior of the material in both temperature and stress (Fig. 6(b)). The specimen's temperature reached a peak/valley at the end of the forward/reverse phase transition. The amount of temperature oscillation is about 22.4 °C and is much higher than that of Fig. 6(a). The average temperature of the specimen is higher than the room temperature but shifted down (for 3–4 °C in the transient stage) and eventually reaches its steady-state value. Because of the temperature dependence of the stress, the corresponding cyclic stress–strain curves became a hardening type and also shifted down in the transient stage and saturated into a repeatable hysteresis loop. The hysteresis loop area is now distorted due to the self-heating (in loading)

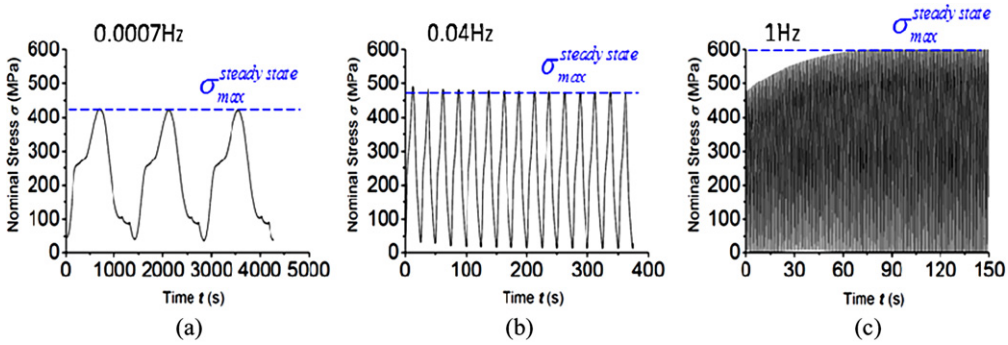

Fig. 7. Stress oscillations corresponding to the temperature oscillations in Fig. 6.

and self-cooling (in unloading) of the material and no longer represents a characteristic property of the material as that in Fig. 6(a).

When the cyclic deformation frequency is increased to 1 Hz, the thermal effect on the cyclic behavior becomes even more significant (Fig. 6(c)). On the one hand, the release/absorption of latent heat causes a near spontaneous temperature increase/decrease of the specimen with the amplitude of 23 °C in temperature oscillation. On the other hand, the released heat from the hysteresis loop of the material has not enough time to transfer out. The hysteresis heat accumulates rapidly in the specimen, causing a large increase in the average temperature up to the saturation value of 61 °C (with the temperature peak of 72.5 °C). In strong contrast to the first mechanism, the corresponding stress–strain curves had a significant hardening, shifted up significantly and eventually reached saturation. As shown in Fig. 7, the stress oscillation had a peak of 600 MPa in the case of 1 Hz in Fig. 6(c) while it is only 420 MPa in the case of 0.0007 Hz in Fig. 6(a). The saturated hysteresis loop area became even smaller due to the strong thermal effect [18,29,30]. From the above experimental observation, the following important features of the material behavior due to the second mechanism can be obtained:

(1) In the cyclic phase transition experiments of the trained specimen under three different frequencies, the residual strain after unloading is very small and ignorable. This demonstrates that the observed thermomechanical response is almost purely caused by the second mechanism. It should be noticed that, in general, there should be no exclusive operation between the first and the second mechanisms. They can both produce the residual strain. Here, in order to clearly differentiate the effects of the two mechanisms, we purposely trained the specimen to remove the major effects of dislocation/plasticity and the caused residual martensite so as to clearly illustrate the second mechanism.
(2) Under cyclic deformation both temperature and stress experience oscillations which have transient stages before they finally reach steady states (thermal shake down). The transient stage of the temperature variation is characterized by the frequency-dependent average temperature change which shifts down at lower frequency and shifts up at higher frequency. The physical origin of the oscillation is the release and absorption of the latent heat from cyclic phase transition. The temperature variation in the transient stage showed strong frequency dependence in reaching the final steady state and reflected the competition of the heat transfer rate and the heat supply rate in reaching the steady state. The material property (such as amount of latent heat, hysteresis heat and heat capacity) and heat transfer condition of the ambient also play important roles in the transient stage.
(3) Following the transient stage is the stage of the steady-state temperature variation where the temperature profile oscillates around the average temperature plateau. The oscillation is mainly due to the release and absorption of the latent heat and the amplitude increases with the loading frequency and eventually reaches saturated value at high frequency (near adiabatic) condition. The value of the steady-state average temperature plateau (i.e., the mean temperature over a cycle) is mainly determined by the accumulation of the hysteresis heat and increases monotonically with frequency without saturation. This is because the higher the frequency, the more rapid the accumulation of heat.
(4) Under cyclic deformation, the stress oscillates at the same pace as the temperature oscillation because of the intrinsically temperature dependence of the stress. The stress oscillation also experiences a transient stage in which the average stress shifts down or up before reaching the steady-state hysteresis loop. There exist the same trends of increases in the average stress with the frequency as that of the temperature. In the present experiment, a cyclic transformation under frequency 1 Hz at room-temperature (∼25 °C) air can bring the specimen's temperature up to 72.5 °C and stress up to 600 MPa. This large stress rise due to the hysteresis heat has not been reported so far and will lead to an unexpected acceleration of degradation and fatigue failure of the material.

To have a quantitative understanding of the roles of the time scale of loading (or the rate of latent heat release and heat accumulation) and the time scale of heat transfer, modeling and analysis on the physical process were performed recently by the authors [22]. The temperature history $T_{av}(t)$ of a NiTi SMA wire (radius r) under displacement-controlled sinusoidal cyclic deformation of frequency $f(=1/t_p)$ was obtained by solving the lumped heat transfer equation [24] of the wire. $T_{av}(t)$ was obtained as, [22]:

$$T_{av}(t) = T_0 + \frac{D_0\bar{t_h}\omega}{2\pi\lambda} + \left(\frac{l_0\bar{t_h}^2\omega^2}{2\lambda(1+\bar{t_h}^2\omega^2)} - \frac{2D_0\bar{t_h}^3\omega^3}{\pi\lambda(1+4\bar{t_h}^2\omega^2)}\right)e^{-\frac{t}{\bar{t_h}}} + \frac{l_0\bar{t_h}\omega}{2\lambda\sqrt{1+\bar{t_h}^2\omega^2}}\sin\left(\omega t - \cos^{-1}\frac{1}{\sqrt{1+\bar{t_h}^2\omega^2}}\right) - \frac{D_0\bar{t_h}\omega}{2\pi\lambda\sqrt{1+4\bar{t_h}^2\omega^2}}\sin\left(2\omega t + \sin^{-1}\frac{1}{\sqrt{1+4\bar{t_h}^2\omega^2}}\right) \tag{3}$$

in which, T_0 is the initial temperature at $t = 0$, ω is the angular frequency ($\omega = 2\pi f$) of cyclic deformation, $\bar{h}$ is the lumped effective heat convection coefficient with the external ambient, $\bar{t_h}(= \frac{r\lambda}{\bar{h}})$ is the lumped characteristic relaxation time of the effective heat convection, l_0 is the latent heat, λ is heat capacity, D_0 is the stress hysteresis loop area in each frequency heat source. The transient stage of temperature variation is determined by the third term in Eq. (3) which well explains the opposite trends of the frequency-dependence in Figs. 6(b) and (c). Let $t \to \infty$, we have the steady-state solution of the temperature variation $T_{av}(t)$ as:

$$T_{av}(t) = \left(T_0 + \frac{D_0\bar{t_h}\omega}{2\pi\lambda}\right) + \frac{l_0\bar{t_h}\omega}{2\lambda\sqrt{1+\bar{t_h}^2\omega^2}}\sin\left(\omega t - \cos^{-1}\frac{1}{\sqrt{1+\bar{t_h}^2\omega^2}}\right) - \frac{D_0\bar{t_h}\omega}{2\pi\lambda\sqrt{1+4\bar{t_h}^2\omega^2}}\sin\left(2\omega t + \sin^{-1}\frac{1}{\sqrt{1+4\bar{t_h}^2\omega^2}}\right) \tag{4}$$

The first term on the right side of the equation represents the steady-state average temperature which increases monotonically with the frequency and is caused by the accumulation of hysteresis heat; the remaining two terms are the temperature oscillations caused by latent heat and hysteresis heat, respectively. From Eqs. (3) and (4), we can clearly see that, in addition to the material properties and parameters, the ratio of the two time scales $\bar{t_h} \cdot \omega$ determines the average temperature and the temperature oscillation. This prediction of the model agrees well with the experimental data [22].

4. Conclusions

In this article, we briefly reported recent advances in investigating the spatiotemporal evolution of deformation and temperature fields in non-equilibrium (i.e., non-isothermal) solid–solid phase transition process in NiTi polycrystalline shape memory alloys. We tried to elucidate the fundamental physics behind the rate-dependent behavior of the material during phase transition and have arrived at the following preliminary conclusions:

- The non-equilibrium phase transition (non-isothermal) of NiTi under uniaxial stretching exhibits a strong rate-dependent spatiotemporal evolution of domain patterns. The domain spacing is not only a measure of the material heterogeneity, but also emerges as a new internal length scale of the material in the stress-induced non-equilibrium phase transition. The domain spacing strongly depends on the applied strain rates or the time scale of phase transition. It was measured in the carefully designed tensile experiment over the strain rate from 10^{-5}/s to 10^{2}/s (the corresponding loading time ranges from 10^{3} s to 10^{-4} s). The results showed that the higher the strain rate, the finer the domain patterns. We further showed that such rate-dependent phenomenon physically originates from the material's nonlinearity (instability of deformation), the non-isothermality of the phase transition process and the coupling between the mechanical and thermal events. Through experiment and analysis, we found that it is the competition among the characteristic time scales of the heat transfer of the system and the time scale of phase transition (loading) that imposes the internal length scale to the meso- and microstructure of an initially macroscopic homogeneous material. Simple scaling law governing the observed rate dependence has been developed and agrees well with the experiments in static air.
- Under displacement-controlled cyclic reversible phase transition (deformation), both temperature and stress experience oscillations which finally reach their steady states through the transient stages. The physical origin of the oscillation is the release and absorption of latent heat from cyclic phase transition, while the average temperature increase in the steady state is due to the accumulation of the hysteresis heat and reflects the final balance between the rate of heat transfer and the rate of heat supply. Both depend on the deformation frequency. The stress oscillates at the same pace as the temperature because the stress is intrinsically temperature-dependent. The stress oscillation and the average stress also increase with the frequency of the temperature. Similar to the temperature oscillation, the stress oscillation also experiences the transient stage in which the average stress shifts down or up before reaching the steady state. Such a heat-induced stress variation plays an important role in the degradation and failure of the material and must be systematically investigated in the future.

Before closing this section, we would like to comment that a fundamental paradigm in materials science and engineering is the structure–property relationship of material. Therefore, understanding and developing quantitative predictive models on formation and evolution of structures constitute central challenges of nowadays micromechanics research since understanding and prediction give the possibility of both structure control and development of new technologies for material synthesis. Microstructure evolution during phase transition has been and will continuously be one of the richest and active areas of micromechanics. The challenges to the mechanics scientists are to further understand the origins of such

heterogeneities, quantify the observed phenomena, and to control the processes so as to obtain optimized microstructure with desired property on demand. The research of this area is very broad and poses a variety of opportunities for the micromechanics community where André Zaoui has contributed significantly. The door is widely open.

Acknowledgements

The authors would like to acknowledge the Hong Kong Research Grant Council for the financial support of this work under project No. 620109.

References

[1] J.P. Gollub, J.S. Langer, Pattern formation in nonequilibrium physics, Review of Modern Physics 71 (1999) S396–S403.
[2] M.C. Cross, P.C. Hohenberg, Pattern formation outside of equilibrium, Review of Modern Physics 65 (1993) 851–1047.
[3] J.S. Langer, Instabilities and pattern formation in crystal growth, Review of Modern Physics 52 (1980) 1.
[4] J.A. Shaw, S. Kyriakides, Thermomechanical aspects of NiTi, Journal of the Mechanics and Physics of Solids 43 (1995) 1243–1281.
[5] J.A. Shaw, S. Kyriakides, On the nucleation and propagation of phase transformation fronts in a NiTi alloy, Acta Materialia 45 (1997) 683–700.
[6] O.P. Bruno, P.H. Leo, F. Reitich, Free boundary conditions at austenite–martensite interfaces, Physical Review Letters 74 (1995) 746–749.
[7] L.C. Brinson, I. Schmidt, R. Lammering, Stress-induced transformation behavior of a polycrystalline NiTi shape memory alloy: micro and macromechanical investigations via in situ optical microscopy, Journal of the Mechanics and Physics of Solids 52 (2004) 1549–1571.
[8] C.B. Churchill, J.A. Shaw, M.A. Iadicola, Tips and tricks for characterization shape memory alloy wire: Part 3 – Localization and propagation phenomena, Experimental Techniques 33 (2009) 70–78.
[9] W.M. Huang, Bin Yang, Yong Qing Fu, Polyurethane Shape Memory Polymers, CRC Press, 2011.
[10] Q.P. Sun, Z.J. Zhao, W.Z. Chen, X.L. Qing, X.J. Xu, F.L. Dai, Experimental study of stress-induced localized transformation plastic zones in tetragonal zirconia polycrystalline ceramics, Journal of the American Ceramic Society 77 (1994) 1352–1356.
[11] D. Favier, H. Louche, P. Schlosser, L. Orgeas, P. Vacher, L. Debove, Homogeneous and heterogeneous deformation mechanisms in an austenitic polycrystalline Ti-50.8 at.% Ni thin tube under tension. Investigation via temperature and strain fields measurements, Acta Materialia 55 (2007) 5310–5322.
[12] L. Dong, Q.P. Sun, On equilibrium domains in superelastic NiTi tubes – helix versus cylinder, International Journal of Solids and Structures (2012), in press, http://dx.doi.org/10.1016/j.ijsolstr.2012.01.006.
[13] C. Grabe, O.T. Bruhns, On the viscous and strain rate dependent behavior of polycrystalline NiTi, International Journal of Solids and Structures 45 (2008) 1876–1895.
[14] M.A. Iadicola, J.A. Shaw, Rate and thermal sensitivities of unstable transformation behavior in a shape memory alloy, International Journal of Plasticity 20 (2004) 577–605.
[15] P.H. Leo, T.W. Shield, O.P. Bruno, Transient heat transfer effects on the pseudoelastic behavior of shape-memory wires, Acta Metallurgica et Materialia 41 (1993) 2477–2485.
[16] K.L. Ng, Q.P. Sun, Stress-induced phase transformation and detwinning in NiTi tubes, Mechanics of Materials 38 (2006) 41–56.
[17] Y.J. He, Q.P. Sun, Rate dependence of domain spacing in phase transition under tension, International Journal of Solids and Structures 47 (2010) 2775–2783.
[18] Y.J. He, H. Yin, R.H. Zhou, Q.P. Sun, Ambient effect on damping peak of NiTi shape memory alloy, Materials Letters 64 (2010) 1483–1486.
[19] E.A. Pieczyska, S.P. Gadaj, W.K. Nowacki, H. Tobushi, Investigation of nucleation and propagation of phase transitions in TiNi SMA, QIRT Journal 1 (2004) 117–128.
[20] E.A. Pieczyska, S.P. Gadaj, W.K. Nowacki, Phase-transformation fronts evolution for stress- and strain-controlled tension tests in TiNi shape memory alloy, Experimental Mechanics 46 (2006) 531–542.
[21] X.H. Zhang, P. Feng, Y.J. He, T.X. Yu, Q.P. Sun, Experimental study on rate dependence of macroscopic domain and stress hysteresis in NiTi shape memory alloy strips, International Journal of Mechanical Science 52 (2010) 1660–1670.
[22] H. Yin, PhD thesis, Hong Kong University of Science and Technology, 2012.
[23] R. Zhou, PhD thesis, Hong Kong University of Science and Technology, 2011.
[24] R.M. Cotta, M.D. Mikhailov, Heat Conduction – Lumped Analysis, Integral Transforms, Symbolic Computation, John Wiley and Sons, 1997.
[25] V. Torra, C. Auguet, A. Isalgue, F.C. Lovey, A. Sepulveda, H. Soul, Metastable effects on martensitic transformation in SMA: Part VIII – Temperature effects on cycling, Journal of Thermal Analysis and Calorimetry 102 (2) (2010) 671–680, doi:10.1007/s10973-009-0613-3.
[26] P. Wollants, M. De Bonte, J.R. Roos, Thermodynamic analysis of the stress-induced martensitic-transformation in a single-crystal, Zeitschrift fur Metallkunde 70 (1979) 113–117.
[27] P. Feng, Q.P. Sun, Experimental investigation on macroscopic domain formation and evolution in polycrystalline NiTi microtubing under mechanical force, Journal of the Mechanics and Physic of Solids 54 (2006) 1568–1603.
[28] Q.P. Sun, Y.J. He, A multiscale continuum model on the grain size dependence of the stress hysteresis in shape memory alloy polycrystals, International Journal of Solids and Structures 45 (2008) 3868–3896.
[29] Y.J. He, Q.P. Sun, Frequency-dependent temperature evolution in NiTi shape memory alloy under cyclic loading, Smart Materials and Structures 19 (2010) 115014.
[30] Y.J. He, Q.P. Sun, On non-monotonic rate dependent hysteresis, International Journal of Solids and Structures 48 (2011) 1688–1695.
[31] S. Miyazaki, T. Imai, Y. Igo, K. Otsuka, Effect of cyclic deformation on the pseudoelasticity characteristics of Ti-Ni alloys, Metallurgical and Materials Transactions A 17 (1986) 115–120.
[32] K. Otsuka, C.M. Wayman, Shape Memory Materials, Cambridge University Press, 1998.